Wang *et al. Biochar* (2024) 6:4
https://doi.org/10.1007/s42773-023-00295-x

Biochar

ORIGINAL RESEARCH Open Access

Fe/BC co-conditioners with environmental and economic benefits on composting: reduced NH_3 emissions and improved fertilizer quality

Jixiang Wang[1,2†], Huifang Xie[2†], Jun Wu[3], Weijiang He[1,2], Xi Zhang[1], Junxia Huang[2], Yanfang Feng[1*] and Lihong Xue[1]

Abstract

The significant volatilization of NH_3 during aerobic composting causes nitrogen (N) losses and environmental risks. Both iron (Fe) and biochar (BC) can influence the N conversion process in composting. Fe application can delay the maturation of materials, while biochar can enhance the quality of organic fertilizer. The combination of these two conditioners may help decrease NH_3 emissions and improve organic fertilizer quality. Therefore, this study investigates the effects of different doses of $FeCl_3$ and BC on NH_3 emissions and organic fertilizer quality during composting. The results demonstrated that Fe/BC co-conditioners reduced the accumulation of NH_3 emissions during composting by 11.1–48.2%, increased the total nutrient content by 0.6–15.3%, and enhanced economic and environmental benefits by 0.1–23.6 \$ t^{-1}. At the high-temperature stage of composting, Fe/BC co-conditioners decreased the pH by 0.3–1.2, but there was no significant difference compared to the control at the end of composting, and they did not affect compost maturation. The structural equation model analysis suggested that the reduction in NH_3 emissions was related to ammonia-oxidizing bacteria (AOB), NH_4^+–N, and total nitrogen (TN). As a result, the Fe/BC co-conditioners reduced NH_3 emissions by lowering the pH at the beginning of composting and increasing the content of NH_4^+–N. This study concludes that Fe/BC co-conditioners could complement each other to significantly reduce NH_3 emissions and improve the quality of organic fertilizers.

Highlights

- Different doses of ferric chloride and biochar (Fe/BC) were used for aerobic composting.
- Fe/BC co-conditioning composting significantly reduced NH_3 volatilization.
- Fe/BC co-conditioning composting enhanced N retention and total nutrients.
- NH_3 emission reduction was mainly related to AOB, NH_4^+–N and TN during composting.
- Fe/BC co-conditioning composting could enhance economic and environmental benefits.

Keywords Aerobic composting, Biochar, Organic fertilizer, NH_3 emissions, $FeCl_3$

† Jixiang Wang and Huifang Xie authors contribute to this paper equally.

Handling editor: Xiangzhou Yuan.

*Correspondence:
Yanfang Feng
jaasfengyanfang@163.com; yfeng@jaas.ac.cn
Full list of author information is available at the end of the article

Graphical Abstract

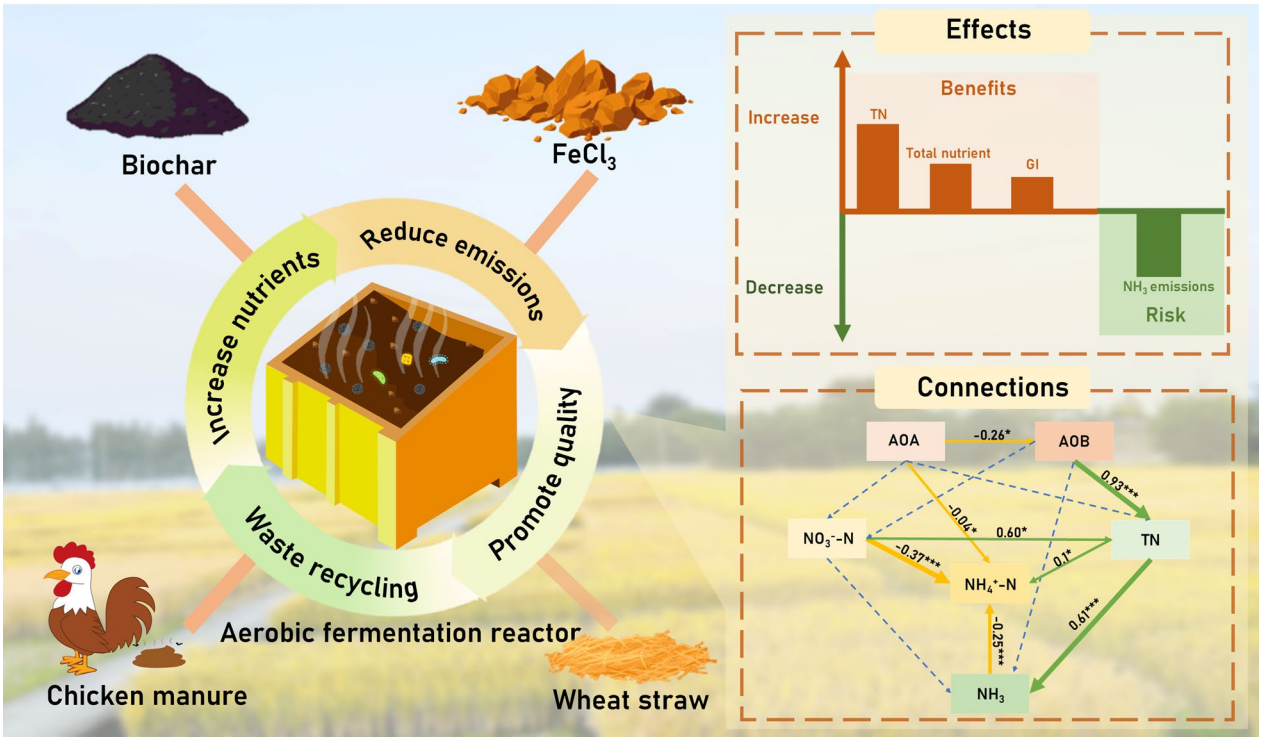

1 Introduction

Aerobic composting is a process in which microorganisms decompose organic waste, converting it into humus, which can be directly used as fertilizer for the fields (Qian et al. 2014). However, this composting process generates a large amount of volatile gas, primarily NH_3, due to biochemical reactions. The volatilization of ammonia not only results in significant nitrogen (N) loss but also contributes to air pollution. Studies indicate that approximately 60% of N loss during aerobic composting is due to NH_3 emissions (Yang et al. 2020). Thus, controlling NH_3 emissions during composting is crucial for reducing environmental risks and improving compost quality.

NH_3 emissions during composting are mainly influenced by factors such as temperature (Kianirad et al. 2010), pH (Cao et al. 2020), moisture content (Ding et al. 2019), aeration rate (Zhang et al. 2013), and C/N ratio (Jiang et al. 2011). Adjusting composting materials, environmental conditions, and process parameters can be costly and challenging. Presently, using conditioners offers clear advantages in reducing N loss during composting. Conditioners come in various forms, including biological, physical, and chemical conditioners (Shan et al. 2021). Biological conditioning involves adding microbial agents during composting, such as high-temperature ammonia-resistant (TA T105H) (Kuroda et al. 2015) and ammonia-oxidizing bacteria (AOB) (Zhang et al. 2016). These microbial inoculants reduce NH_3 emissions by promoting NH_4^+ assimilation or nitrification and lowering NH_4^+ levels (Cao et al. 2019). However, the choice of suitable microbial inoculants depends on the composting materials and parameters.

Physical conditioning involves adding materials with good pore structure, like biochar and zeolite, to adsorb and immobilize NH_3. Biochar is a popular physical conditioner due to its large pore structure and abundant surface functional groups (Liu et al. 2017). Yet, its ability to continuously adsorb NH_3 may be affected by the saturation of adsorption sites. Chemical conditioning focuses on adjusting the pile's pH and the conversion of carbon and nitrogen by adding additives like superphosphate and phosphogypsum. Chemical conditioning is more effective than biological or physical conditioning in reducing NH_3 emissions (Cao et al. 2019). However, the use of chemical conditioners may lead to increased reactor conductivity, incomplete

decomposition, and inhibition of seed germination (Wang et al. 2020).

The effect of iron conditioners on composting has garnered significant attention in recent years. Several studies have demonstrated the effectiveness of iron conditioners in reducing NH_3 emissions during composting. For instance, Liu et al. (2022) found that 3% zero-valent iron (ZVI) effectively reduced NH_3 cumulative emissions by 9.4% in sludge composting. Similarly, Chen et al. (2022) reported that the addition of 5% $FeSO_4$ reduced NH_3 emissions by 12.4% during pig manure composting. Despite their efficacy, these iron conditioners have limited practical applications due to their poor stability. $FeCl_3$, a common acidic salt material with good stability, presents a potential alternative for reducing NH_3 emissions during composting. In recent years, researchers have rarely studied ferric chloride as an aerobic regulator. And little is known about the changes in physicochemical properties and the effect of NH_3 emissions in composting with the addition of $FeCl_3$. Therefore, it is necessary to investigate the effect of adding $FeCl_3$ on the composting process. However, adding $FeCl_3$ alone may result in a high concentration of salt ions in the compost, which can impact material maturation and adversely affect seed germination. To address this issue, the addition of biochar conditioner, which possesses a buffering effect and reduces phytotoxicity in composting, could prove beneficial. Combining $FeCl_3$ and biochar may be more effective in reducing NH_3 emissions. In recent years, the use of $FeCl_3$ and the combination of $FeCl_3$ and biochar as a compost conditioner has not been reported yet. The mechanisms of their effects on the physicochemical characteristics and NH_3 emissions of the composting process deserve to be explored by researchers.

In this study, the researchers hypothesize that co-conditioning aerobic composting with Fe/BC could lead to complementarity between the two additives, resulting in significantly reduced NH_3 emissions and improved organic fertilizer quality. The objectives of the study were (a) to investigate the effects of $FeCl_3$ and biochar on NH_3 emissions during aerobic composting and analyze the potential mechanism behind emissions reduction; and (b) to examine the physical and chemical properties, nutrient dynamics, organic matter, and humus content of the Fe/BC composting process and further evaluate its overall impact on the quality of organic fertilizer. Through this research, the study aims to present a new approach for reducing the risk of NH_3 emissions and enhancing the quality of organic fertilizers in the composting process by utilizing Fe/BC co-conditioners.

2 Materials and methods

2.1 Experimental materials

The main ingredients used in aerobic composting were chicken manure and wheat straw, both of which were collected from a local farm in Nanjing, Jiangsu Province. The wheat straw was cut into small pieces measuring 1–2 cm for better utilization. Additionally, wood biochar was utilized in the composting process, and its preparation involved a temperature of 400 °C, resulting in a biochar with a pH of 7.82, surface area of 6.84 $m^2\ g^{-1}$, total pore volume of 0.018 cc g^{-1}, and an average pore diameter of 8.98 nm. For further details on the properties of the composting materials, please refer to Additional file 1: Table S1 and Fig. S1.

The composting reactor used in this study was comprised of incubators with an outer diameter measuring 64 × 48 × 36 cm. The case's shell and inner liner were constructed from PP material, and the center featured a 5 cm-thick polystyrene foam, providing thermal insulation functionality. To monitor the temperature during composting, an RC-4 automatic thermometer was utilized.

For further analysis of the composting materials, the FI-IR spectra and 2D-COS analysis can be referred to in Additional file 1: Figs. S3 and S4, respectively. These additional figures provide valuable information on the composting process and its materials.

2.2 Treatments

The aerobic composting experiment took place in a greenhouse located at the Jiangsu Academy of Agricultural Sciences (118.87° E, 32.03° N). For the experiment, chicken manure and wheat straw were thoroughly and evenly mixed at a dry weight ratio of 1.5:1. Each composting reactor's initial dry weight of organic waste was 8 kg, with an initial C/N ratio of approximately 20–25, and the initial moisture content was maintained at around 60%. The entire composting experiment spanned a period of 30 d.

To investigate the impact of different additives on the composting process, five distinct treatment groups were established based on different additive ratios (Control group without any conditioner application (CK); F1: Composting with 1% $FeCl_3$ (*w/w*) additive; F3: Composting with 3% $FeCl_3$ (*w/w*) additive; F1 + B15: Composting with a combination of 1% $FeCl_3$ and 15% biochar (BC, *w/w*) as additives; F3 + B15: Composting with a combination of 3% $FeCl_3$ and 15% biochar (BC, *w/w*) as additives).

2.3 Sample collection and analysis

2.3.1 Sample collection

The composting samples were subjected to full turning on the 4th, 7th, 10th, 13th, 17th, and 21st day. A total of 200 g of samples were collected from the center and four corners of the compost pile and mixed thoroughly to ensure homogeneity. Subsequently, 50 g of these samples were transported back to the laboratory for testing, while the remaining samples were returned to the composting reactor.

Each collected sample was divided into two parts. One part was frozen and stored for later analysis of physical and chemical properties, while the other part was dried and crushed to determine nutrient content, organic matter, and humus levels.

2.3.2 NH3 collection and testing

NH_3 was collected using a closed batch pumping technique with boric acid absorption. The collection setup comprised a sealed plexiglass cylinder with a 10 cm diameter, featuring air inlet and air outlet at the top. The inlet hole was connected to a vent pipe, which extended to a height of 2 m. Additionally, the outlet hole was linked to a vacuum pump through the absorption device. During the composting cycle, NH_3 was collected for a duration of 4 h each day. The collected NH_3 was then titrated using 0.02 mol L^{-1} sulfuric acid, and 2% boric acid was utilized as the absorbent solution. Furthermore, the titration process employed methyl red-bromocresol green as an indicator to detect the endpoint.

2.3.3 Physicochemical index determination

Temperature recording during composting involved inserting a temperature recorder into the center of the compost pile at the beginning of the process. The temperature readings were taken every half hour, throughout the day. To analyze the data, the average temperature of the day was calculated, and the ambient temperature was also measured. Additionally, this data was used to assess the feasibility of collecting ammonia volatilization data in the system. The effective accumulated temperature equation is as follows:

$$T = \Sigma(T_i - T_0) \times \Delta t \quad (1)$$

where T_i is the pile temperature at the moment i, T_0 is the initial temperature (biological zero) at the time of microbial proliferation in the compost, and Δt is the duration of Ti.

Determination of pH, EC, and GI: Fresh composting samples were mixed with deionized water at a ratio of 1:10 (solid–liquid ratio). The mixture was then oscillated for 30 min to ensure proper mixing. After oscillation, the mixture was left to stand for 10 min to allow any solid particles to settle. Subsequently, the supernatant was collected for further testing. The collected liquid sample was used to measure the pH and EC. This was accomplished using a multi-parameter analyzer. According to Shan et al. (2019), the GI (Germination Index) was measured and calculated using the following formula:

$$GI(\%) = \frac{Seed\ germianation(\%) * root\ length\ of\ treatment}{Seed\ germianation(\%) * root\ length\ of\ control} * 100\% \quad (2)$$

2.3.4 Nutrient determination

Determination of NH_4^+–N and NO_3^-–N: Fresh compost samples and 2 mol L^{-1} KCl solution were mixed in the ratio of 1:10 (*w/v*). The samples were shaken for 30 min and allowed to stand for 10 min for filtration. The filtrate was analyzed using a flow analyzer, and a total of 3 replicates were performed.

Determination of TN, TP, and TK: The H_2SO_4-H_2O_2 method was employed to process the composting samples. Subsequently, the total nitrogen content of the processed samples was determined using a Kjeldahl nitrometer. Additionally, the total phosphorus (P) and potassium (K) levels were analyzed using inductively coupled plasma optical emission spectroscopy (ICP-OES, Optima TM8000, Perkin Elmer) (Bartos et al. 2014).

2.3.5 Determination of organic matter and humus

Determination of Humus (HS) Content: A 2.50 g air-dried compost sample was taken and added to sodium hydroxide and disodium hydrogen phosphate extract. The resulting supernatant was collected to determine total organic carbon (TOC), representing the total humus content. From this, 20.00 mL of the supernatant was taken and 6 mol L^{-1} HCl was added to precipitate the solution. The resulting supernatant contained fulvic acid (FA), while the precipitated substance was humic acid (HA). The content of fulvic acid (FA) was determined using a TOC instrument, and the humic acid content was obtained by calculating the difference between the total humus content and the fulvic acid content (Wang et al. 2016).

Determination of Organic Matter (OM): The organic matter (OM) content of the composting material was determined using the potassium dichromate volumetric method. Additionally, the dissolved organic carbon (DOC) was measured using an organic carbon analyzer (Wang et al. 2016).

Determination of Dissolved Organic Matter (DOM): To analyze the different types of DOM, 5 g of compost

samples were dissolved in 50 mL of deionized water (*w/v*) and then subjected to centrifugation for filtration (Usman et al. 2019). The 3D-EEM technique was employed with emission wavelengths (Em) and excitation wavelengths (Ex) ranging from 200 to 900 nm. Three parameters of the fluorescence spectrum were analyzed: fluorescence index (FI), biological index (BIX), and humification index (HIX).

2.3.6 Quantitative PCR of AOA-amoA and AOB-amoA gene

DNA Extraction and Quantification: DNA was extracted from a 0.25 g compost sample and quantified using fluorescence quantitative PCR (ABI7500, Applied Biosystems, USA). For the AOA-amoA gene, the upstream primer was "STAATGGTCTGGGCTTAGACG," and the downstream primer was "GCGGCCATCCATCTGTATGT." For the AOB-amoA gene, the upstream primer was "GGGGTTTCTACTGGTGGGT," and the downstream primer was "CCCCTCKGSAAAGCCTTCTTC."

qPCR Amplification Conditions: The qPCR amplification was conducted with the following conditions:

1. Pre-denaturation at 94 °C for 15 min.
2. Cycles: a. Denaturation at 94 °C for 30 s, b. Annealing at 55 °C for 30 s, c. Extension at 55 °C for 30 s, d. Final extension at 55 °C for 30 s.
3. Extension at 72 °C for 10 min.

Quantification of Copy Number: The copy number of each DNA sample was determined using the amplification standard curve method.

2.3.7 Statistical analysis

Microsoft Excel (2022) was utilized for data processing, while SPSS 27 was employed for conducting statistical analysis. Univariate analysis of variance (ANOVA) was used to calculate the significant differences ($P < 0.05$). The image was created using Origin (2023b). The 3D-EEM images were generated using the R language. The models were validated through disassembly analysis, model fitting, and visual inspection of residuals.

3 Results and discussion

3.1 *NH_3 emissions during Fe/BC co-conditioning composting*

Figure 1a illustrates the daily curve of NH_3 emissions during composting. The composting process encompassed three distinct stages: high-temperature period (HTP, Days 1–7), cooling period (CP, Days 8–19), and maturation period (MP, Days 20–28). Notably, NH_3 emissions exhibited a fluctuating pattern in response to reactor turning. During the high-temperature period,

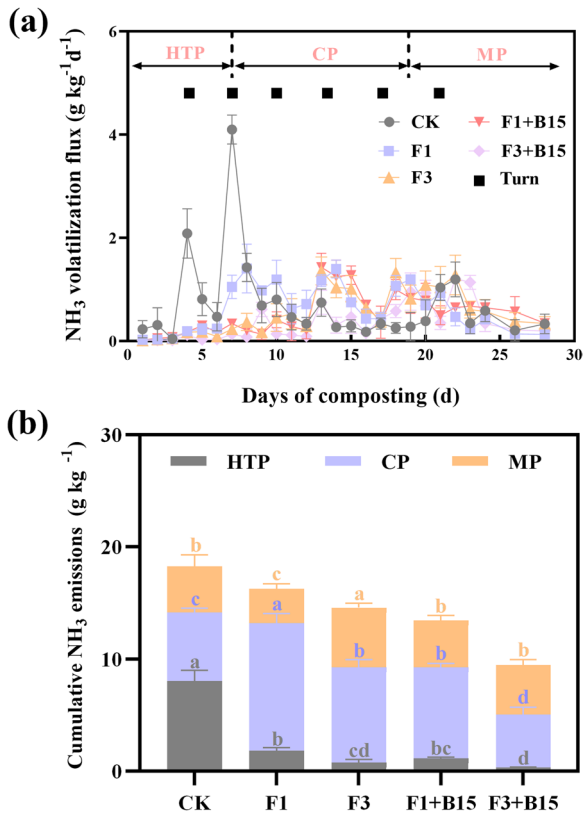

Fig. 1 **a** Daily ammonia emissions during composting; **b** cumulative ammonia emissions at the end of composting. *HTP* High temperature period, *CP* cooling period, *MP* maturation period, *Turn* Turn the composting samples. Data are mean ± SD (n = 4)

microorganisms effectively degraded amino acids, proteins, and other readily degradable organic matter, leading to the production of NH_3. The CK treatment experienced its peak NH_3 emissions primarily in the high-temperature period of composting, with a peak intensity of 4.10 g kg^{-1} d^{-1}, consistent with conventional aerobic composting trends (Zhang et al. 2014). On the other hand, for the F1, F3, F1 + B15, and F3 + B15 treatments, the peak NH_3 emissions were more pronounced during the cooling period, with the F1 + B15 treatment demonstrating the highest peak intensity (1.43 g kg^{-1} d^{-1}). Remarkably, these treatments exhibited a significant reduction in peak NH_3 emissions (65.1–72.2%) compared to the CK treatment. This outcome aligns with the findings of Chen et al. (2022), who observed a similar reduction in NH_3 emissions (43.7%) and TN loss (33.8%) upon the addition of 5% $FeSO_4$. The decrease in NH_3 emissions can be attributed to the pH-lowering effect of the Fe conditioner during the composting process, along with the increased NH_4^+–N content in the high-temperature period, which effectively curtails NH_3 emissions.

Figure 1b displays the cumulative NH_3 emissions during composting. Regarding the NH_3 cumulative emissions during the high-temperature period of composting, the CK treatment exhibited the highest NH_3 cumulative emissions, while the other treatments showed reductions ranging from 77.3% to 95.7% compared to the CK treatment. In terms of NH_3 cumulative emissions during the cooling period of composting, the F1, F3, and F1 + B15 treatments recorded higher NH_3 cumulative emissions than the CK treatment. Notably, among these, the F1 treatment had the highest cumulative emissions of NH_3, measuring 11.40 g kg^{-1}, accounting for 70.1% of the cumulative emissions of NH_3 throughout the treatment cycle. In relation to NH_3 cumulative emissions during composting maturity, the F3 treatment exhibited the highest NH_3 cumulative emissions, reaching 5.33 g kg^{-1}. Additionally, the cumulative NH_3 emissions for each treatment were lower than those during the cooling period.

Considering the cumulative emissions throughout the entire composting cycle, the F1, F3, F1 + B15, and F3 + B15 treatments demonstrated significant reductions ranging from 11.1% to 48.2% in NH_3 emissions compared to the CK treatment. The NH_3 emissions reduction effect was more pronounced in the F3 treatment compared to the effect observed in the case of the F1 treatment, suggesting a positive correlation between the amount of $FeCl_3$ addition and NH_3 emissions. Presumably, higher $FeCl_3$ levels were more effective in reducing pH levels and retaining NH_4^+. Moreover, the F3 + B15 treatment exhibited the greatest potential in reducing NH_3 emissions during composting. Apart from the role of $FeCl_3$ in NH_3 emissions reduction, biochar also played a significant role, owing to its unique porous structure and extensive specific surface area, which facilitated the absorption of NH_3 released during composting (Xiao et al. 2017). Furthermore, biochar influenced NH_4^+–NH_3 balance and nitrogen mineralization dynamics, thereby contributing to the reduction of NH_3 emissions (Awasthi et al. 2017).

3.2 Physicochemical properties during Fe/BC co-conditioning composting

3.2.1 Composting temperature

Temperature is a key parameter in the process of aerobic composting (Greff et al. 2022), and its temperature change will affect the activity of different kinds of microorganisms, thus affecting the decomposition rate of organic matter.

The temperature variation trend of each treatment was basically the same (Fig. 2a). All treatments heated up rapidly on the first day of composting. When the temperature reaches 50 °C, it can be considered to enter the HTP. In this stage, thermophilic microorganisms decompose complex organic matter (cellulose, protein, etc.) in the material, resulting in the continuous rise of the compost temperature (Sudharsan Varma and Kalamdhad 2015). CK, F1, F3, F1 + B15 and F3 + B15 maintained above 50 °C for 6–7 days. The peak temperature of each treatment was 60.0–69.0 °C, and then the temperature began to decrease gradually, and finally the temperature gradually stabilized at 26.2–29.2 °C. The peak temperature of F3 and F3 + B15 treatments in the high temperature stage of composting was significantly lower than that of other treatments, and the time of entering the high temperature stage was significantly delayed. After the first 4 turns (on Day 4, 7, 10, 13, respectively), the temperature of each treatment showed a rapid rise. This is mainly due to the increase of oxygen content in the composting after turning over, which is conducive to the growth and reproduction of microorganisms. The temperature of each treatment had no significant change after the last two turns (on Day 17 and 21 respectively).

Figure 2b shows the accumulated temperature during composting. The effective accumulated temperature of all treatments exceeded 10,000 °C. Compared with CK, the effective accumulated temperature of F1 + B15 and F3 + B15 increased by 1.4–3.3%. In terms of the high temperature period in the composting process, accumulated temperature of F1 and F1 + B15 treatments decreased slightly compared with CK. However, the accumulated temperature of F3 and F3 + B15 decreased significantly by 17.0% and 13.1%. During the cooling period, the accumulated temperature of F1 treatment decreased, while the accumulated temperature of F1 + B15, F3 and F3 + B15 increased significantly compared with CK, reaching 14.0–49.9%.

3.2.2 Composting pH and EC

The pH value is an important parameter in aerobic composting. The pH will affect the activity of microorganisms and indirectly affect the process of aerobic composting (Chan et al. 2016). The optimal pH range for aerobic compost is 6.5–8.5 (Proietti et al. 2016). The pH of each treatment in the composting process firstly increased and then decreased (Fig. 2c). Compared with CK, the pH values of the other treatment groups were lower in the high temperature period. This is because the hydrolysis of $FeCl_3$ will produce a large amount of H^+, resulting in a significant decrease in the pH value. This may also be the main reason for reducing NH_3 emissions during HTP. However, at the end of composting, the pH of F1 and F3 decreased slightly compared with CK, while pH of F1 + B15 and F3 + B15 increased by 1.5–3.2%, and the difference was significant ($P < 0.05$). The pH value in the maturation period decreased compared with that in the

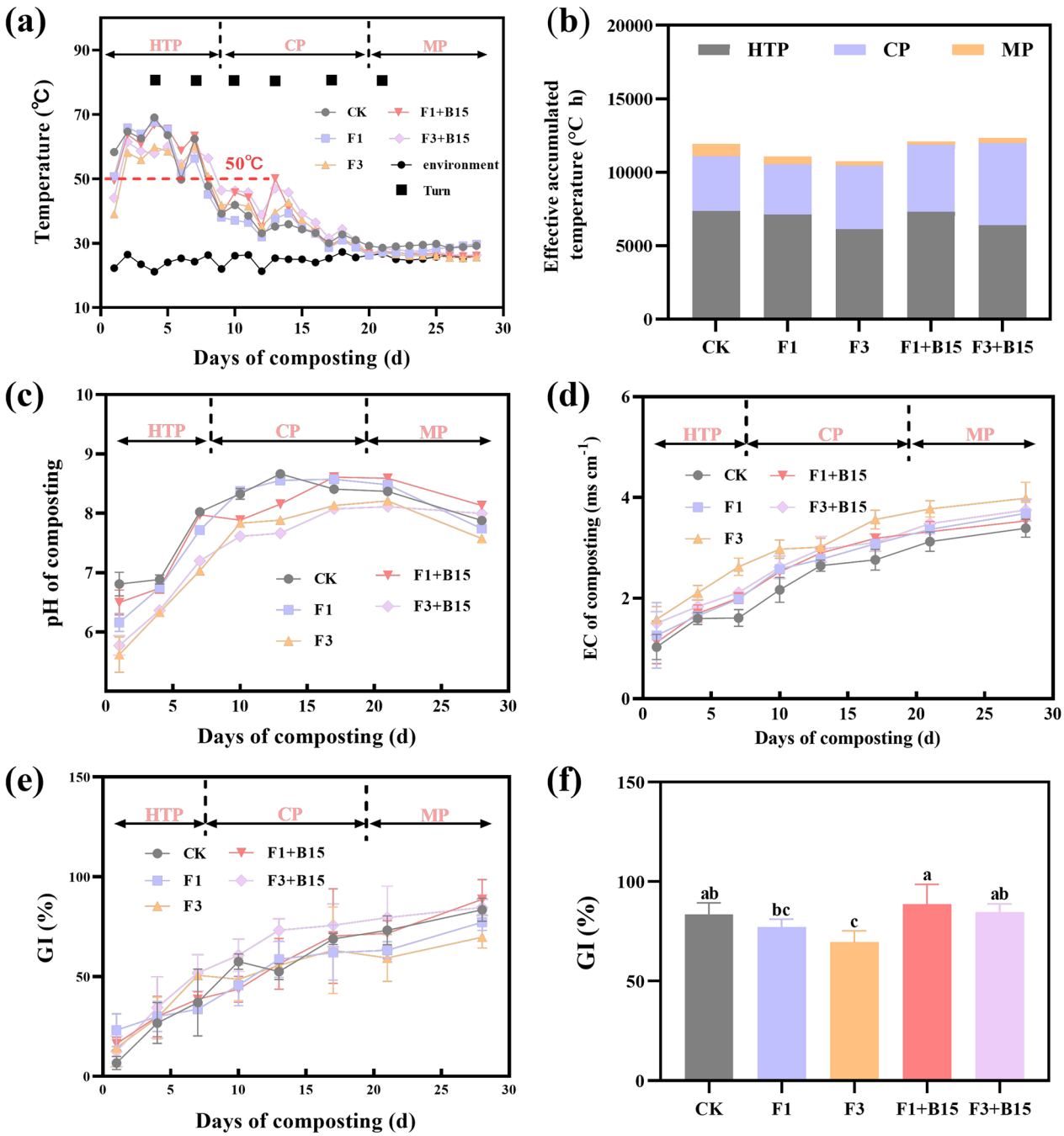

Fig. 2 **a** Daily temperature variation during composting; **b** accumulated temperature of the pile at the end of composting; **c** the pH during composting; **d** the EC during composting; **e** the GI during composting; **f** the GI at the end of the composting; *HTP* high temperature period, *CP* cooling period, *MP* maturation period. Data are mean ± SD (n = 3)

cooling period, which may be related to CO_2 emissions and nitrification process (Liu et al. 2017).

The EC reflects the soluble salt content in the material and indirectly reflects the change of the internal environment of the composting. The EC values for all treatments increased with time from 1.03–1.58 ms cm^{-1} at the beginning to 3.3–3.98 ms cm^{-1} at the end of composting (Fig. 2d). This may be due to the continuous release of soluble salts from the decomposition of organic matter in the composting (Gómez-Brandón et al. 2008). The EC

values of F3 and F3 + B15 treatments were significantly higher than those of other treatments, which may be due to the fact that the introduction of a high amount of $FeCl_3$ will significantly increase the ion content in the composting. The final EC value of F3 + B15 treatment was lower than that of F3 treatment, which was possibly ascribed to the reduction of salt ions by biochar adsorption and mineral salt precipitation processes (Chung et al. 2021).

3.2.3 Germination index (GI)

It is necessary to determine the toxicity of organic fertilizer after composting to determine whether it can be used in agricultural production. Seed germination is the initial stage of plant growth, which can be sensitive to the external growth environment. Therefore, seed germination test is widely used to evaluate the phytotoxicity of compost products and the degree of compost maturation (Yang et al. 2021).

The GI values of all treatments were lower in the early composting stage (Fig. 2e). This is because microbial decomposition of organic matter will produce more ammonium salts and organic acids, and these substances have an inhibitory effect on seed germination. At the same time, the addition of $FeCl_3$ led to a decrease in the pH of the heap, which might also inhibit the germination and growth of plant seeds. With the consumption of organic acids, pH increased and germination index showed a rapid rising trend.

Compared with CK, the GI values of F1 and F3 treatments was reduced to a certain extent, but still higher than 70% in the end, reaching the harmless standard for composting (Fig. 2f). In contrast, the GI value of F1 + B15 and F3 + B15 was 88.7% and 84.7%, respectively, which was higher than that of CK at the end of composting. This is because the added biochar is alkaline and can act as a buffer against the acidity of $FeCl_3$ hydrolysis. Additionally, the content of heavy metal ions, including As, Cd, Cr, and Pb in the final composts was within the standard specified range (Additional file 1: Table S2).

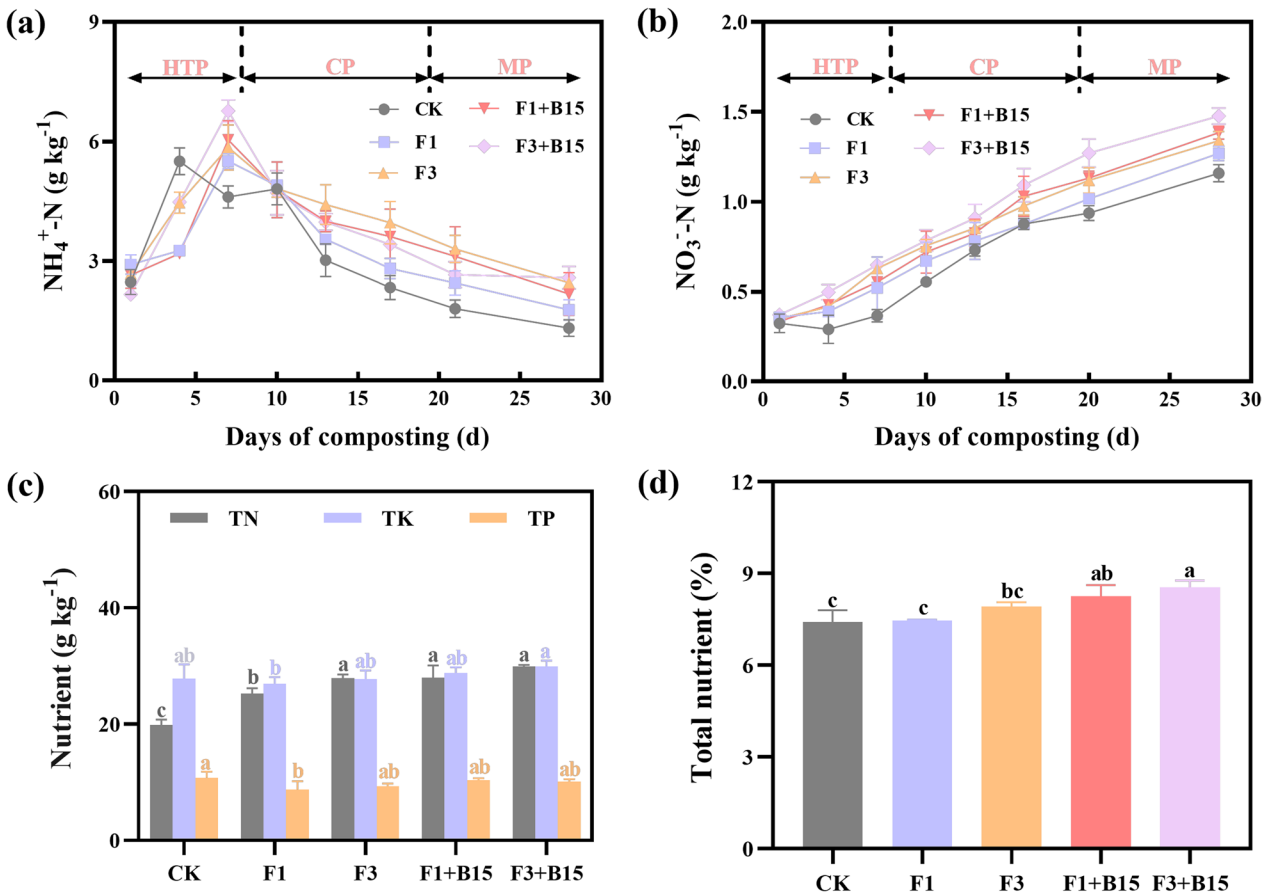

Fig. 3 **a** NH_4^+–N and **b** NO_3^-–N content during composting; **c** TN, TP and TK and **d** total nutrient content at the end of composting; *HTP* high temperature period, *CP* cooling period, *MP* maturation period. Data are mean ± SD (n = 3)

3.3 Nutrient content during Fe/BC co-conditioning composting

3.3.1 $NH4^{+}$–N and NO3−–N content

NH_4^+–N and NO_3^-–N represent essential inorganic nitrogen forms involved in nitrogen conversion during composting. As depicted in Fig. 3a, the NH_4^+-N content in all treatments exhibited an initial increase followed by a subsequent decrease. Upon completion of composting, the F1, F3, F1 + B15, and F3 + B15 treatments displayed significantly higher NH_4^+-N content than the CK treatment, with the F3 + B15 treatment registering the highest levels. This observation can be attributed to the hydrolysis of $FeCl_3$, which creates an acidic environment facilitating NH_3 absorption and consequent NH_4^+–N content enhancement in the composting process (Cao et al. 2020). Moreover, numerous studies have demonstrated that the addition of biochar to composting enhances NH_4^+ adsorption due to its remarkable ion adsorption capability.

The content of NO_3^-–N in all treatments displayed gradually increasing trend, as illustrated in Fig. 3b. After composting, the F1, F3, F1 + B15, and F3 + B15 treatments exhibited an 9.5–27.5% increase in NO_3^-–N content compared to the CK treatment. The low initial pH of the F1, F3, F1 + B15, and F3 + B15 treatments may have inhibited the activity of nitrifying bacteria, contributing to this pattern (Mei et al. 2021). Additionally, nitrate reduction resulted in the transformation of NO_3^-–N into NH_4^+–N, consistent with the changes observed in NH_4^+–N content. Furthermore, the NO_3^-–N content in the F1 + B15 and F3 + B15 treatments surpassed that of the F1 and F3 treatments. The inclusion of biochar increased the porosity of the composting materials and improved oxygen levels within the piles, thereby promoting the nitrification process and leading to the accumulation of NO_3^-–N (Khan et al. 2014).

3.3.2 TN, TP, and TK content

Nitrogen content serves as a critical indicator in composting products. As depicted in Fig. 3c, the TN content underwent significant changes after composting. Comparatively, the TN content in the F1, F3, F1 + B15, and F3 + B15 treatments demonstrated a substantial increase of 27.2–51.1% when compared to the CK treatment ($P < 0.05$). However, there was no significant difference in TK content. The conversion of nitrogen-containing organic matter into nitrogen oxide, accompanied by NH_3 release, played a role in this process. The composting process in F1, F3, F1 + B15, and F3 + B15 treatments experienced an inhibition of microbial activities related to nitrogen decomposition due to the low pH value, leading to a decreased decomposition rate of nitrogen-containing organic materials (Luo et al. 2013). Although TP content in the F1 treatment showed a significant difference compared to CK ($P < 0.05$), no significant difference was observed in TP content in the F3, F1 + B15, and F3 + B15 treatments. Throughout the composting process, phosphorus exhibited relatively greater stability when compared to nitrogen. Despite various forms of phosphorus converting among each other, the absolute content of total phosphorus remained largely unchanged.

In Fig. 3d, the changes in total nutrients after composting were represented. The total nutrient content of compost was determined by calculating the mass fraction of TN + P_2O_5 + K_2O (dry weight). At the end of composting, there was no significant difference in the total nutrient content of the F1 treatment compared to CK. However, the total nutrient content of the F3, F1 + B15, and F3 + B15 treatments demonstrated an increase of 6.8–15.3%.

3.4 Organic matter and humus content during Fe/BC co-conditioning composting

3.4.1 Organic matter content

During the composting process, microorganisms continuously decompose organic matter, leading to a gradual decline in organic matter content (Awasthi et al. 2016). After composting, the organic matter content in the CK treatment was the highest, reaching 65.8% (Fig. 4a). In comparison, the organic matter content in the F1, F3, F1 + B15, and F3 + B15 treatments exhibited a slight reduction when compared to CK. This finding suggests that the addition of Fe/BC improved the final degree of organic matter degradation, which aligns with results obtained by Sudharsan Varma and Kalamdhad (2015).

Figure 4b displays the content of DOC at the end of composting. Throughout the composting process, microorganisms mineralize organic carbon to acquire energy for their growth and reproduction (Wong and Fang 2000). The content of DOC in each treatment exhibited significant changes after composting. Compared to the CK treatment, the content of DOC in the F1, F3, F1 + B15, and F3 + B15 treatments underwent a significant reduction of 33.1–62.1%. It is plausible that the Fe/BC co-conditioner enhanced the porosity of the composting piles, thereby promoting microbial activity. Consequently, the readily degradable part of organic matter, represented by DOC, was swiftly transformed and degraded under the influence of microorganisms, resulting in a substantial decrease in its content (Wang et al. 2016).

3.4.2 Humus content

Humic substances (HS) are types of polymer compounds formed by organic substances under the influence of microorganisms and enzymes, mainly consisting of

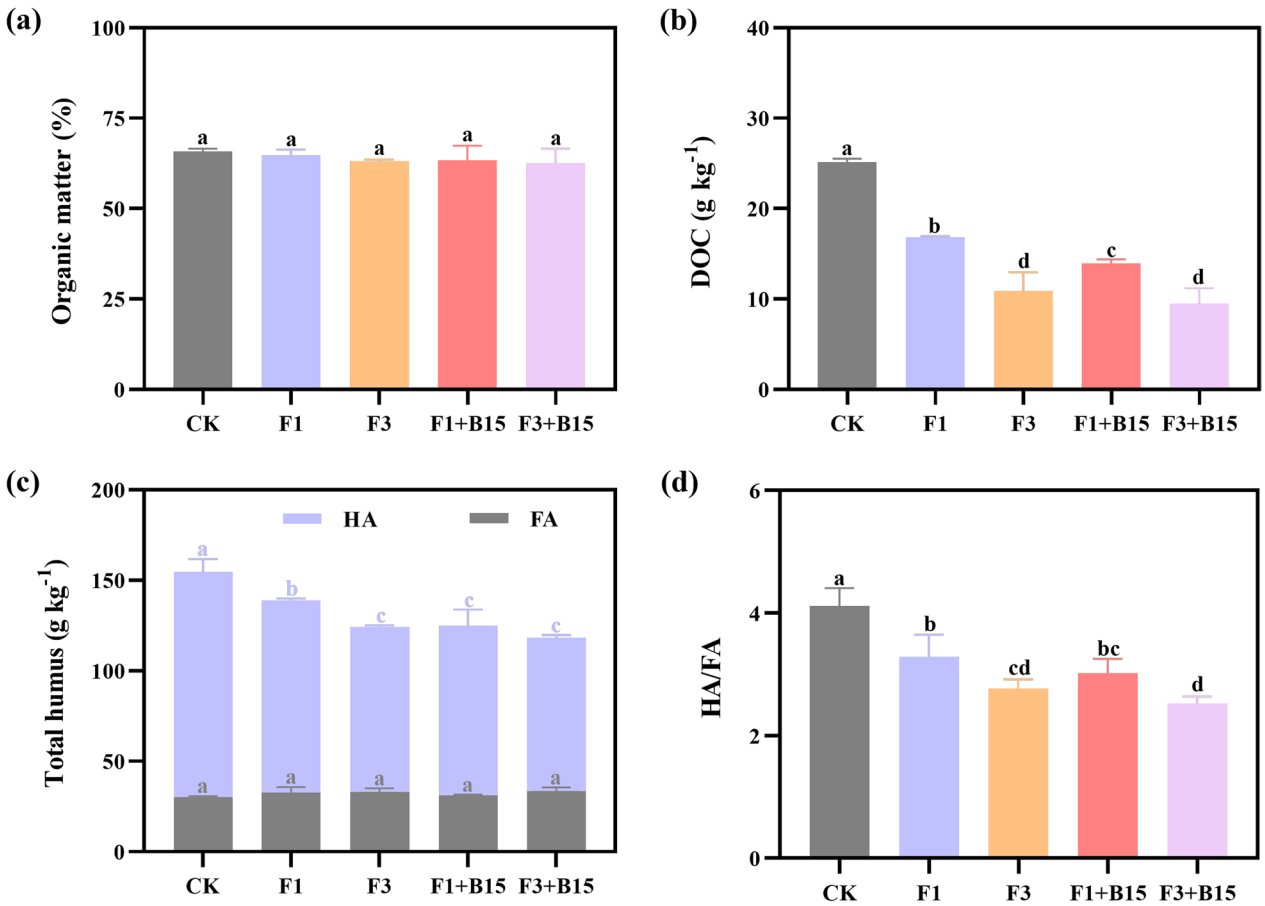

Fig. 4 **a** Organic matter and **b** DOC content at the end of composting; **c** total humus content at the end of composting; **d** HA/FA ratio at the end of composting. Data are mean ± SD (n = 3)

humic acid (HA) and fulvic acid (FA). In aerobic composting, the goal is to obtain highly humified compost products within a short period. The formation and quantity of HS not only reflect the degree of humification of compost products but also indicate the intensity of biodegradation and the stability of the compost (De Melo et al. 2016). After composting, the HS content in the CK treatment was 154.8 g kg^{-1}, whereas, in the F1, F3, F1 + B15, and F3 + B15 treatments, it significantly decreased to a range of 118.4–138.9 g kg^{-1} (Fig. 4c).

HA contains more aromatic carbon and represents a macromolecular organic substance soluble in dilute alkali but insoluble in dilute acid (Li et al. 2021). At the end of composting, the content of HA in the F1, F3, F1 + B15, and F3 + B15 treatments decreased by 14.6–31.9% compared to the control, and this difference was statistically significant ($P < 0.05$). This suggests that the addition of Fe/BC did not favor HA formation. Fe^{3+} readily chelates with hydroxyl, carboxyl, and other functional groups in HA, leading to the formation of stable chelating structures, which consequently decreases the content of HA in the compost (Karlsson and Persson 2012).

On the other hand, FA, as one of the components of humus substances, possesses a smaller molecular weight, higher activity, and greater degree of oxidation compared to HA (Shi et al. 2020). Contrary to CK, the content of FA in the F1, F3, F1 + B15, and F3 + B15 treatments increased by 2.6–10.9% at the end of composting, but there were no significant differences in FA content among the treatments. This indicates that the addition of Fe/BC had limited effects on the activity of microorganisms involved in FA formation and decomposition.

HA/FA ratio serves as an indicator to assess the degree of maturation. A value greater than 1.7 suggests that the pile is essentially decomposed, with higher values indicating a higher degree of humus in the compost (Shan et al. 2013). In this study, the HA/FA of the F1, F3, F1 + B15, and F3 + B15 treatments decreased by 20.0–38.4% compared to CK, with the lowest HA/FA (2.5) observed in

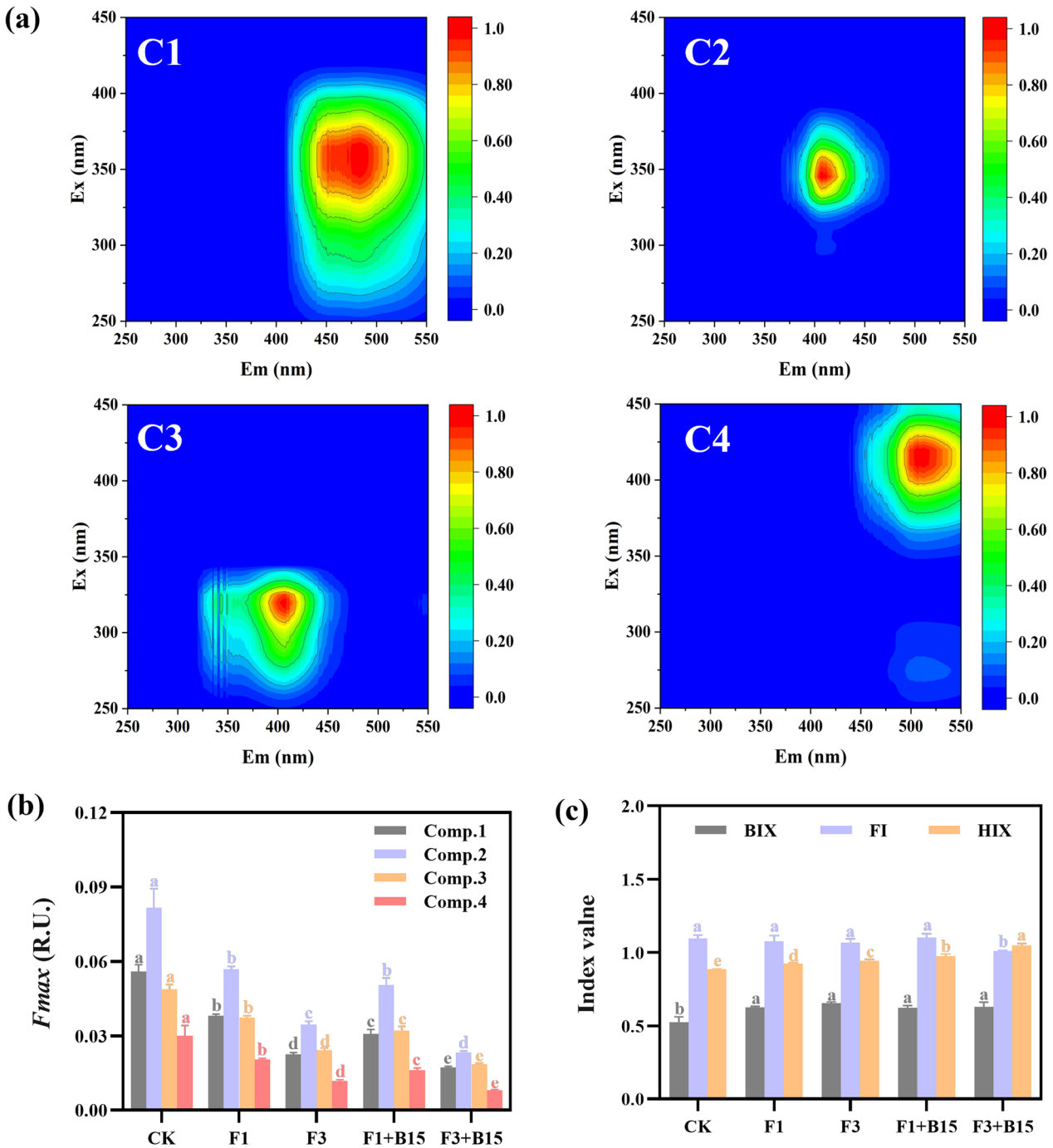

Fig. 5 **a** The fluorescence spectra of dissolved organic matter of composting samples; **b** the maximum fluorescence intensity of four fluorescent components of dissolved organic matter (*Fmax*); **c** the fluorescence parameter of dissolved organic matter. *BIX* Biotic index, *FI* fluorescence index, *HIX* humification index. Data are mean ± SD (n = 3)

the F3 + B15 treatment (Fig. 4d). These findings indicate that the humification of organic matter was achieved in all treatments, while the addition of Fe/BC had a somewhat negative effect on humification to some extent.

3.4.3 Dissolved organic matter fluorescence spectra analysis

The composting process's stability can be partially inferred from the changes in DOM content (Smebye et al. 2016). The fluorescence spectrum of DOM in

composting was obtained through PARAFAC analysis (Fig. 5a). The results revealed four distinct components: Component 1 (C1) represented terrestrial humus with excitation (Ex) and emission (Em) wavelengths around 365 nm and 464 nm, respectively. Component 2 (C2) displayed wavelengths of approximately 340/402 nm at Ex/Em, resembling marine humus but likely derived from land-based organic matter. Component 3 (C3) shared similarities with aromatic compounds, with a peak Ex/Em value of about 305/400 nm. Component 4 (C4) exhibited similarities with FA (Fulvic Acid) with a peak Ex/Em value of around 420/488 nm. Additionally, quantitative PARAFAC analysis was conducted on composting samples under different treatments (Additional file 1: Fig. S2).

In Fig. 5b, the DOM content of F1, F3, F1 + B15, and F3 + B15 treatments decreased significantly by 29.3–68.8% ($P < 0.05$) compared to the CK group, with the most substantial decrease observed in the F3 + B15 treatment. This decline may be attributed to Fe/BC promoting the chemical decomposition of DOM or molecular polymerization, leading to the formation of macromolecular humus (López-González et al. 2013).

Furthermore, the addition of $FeCl_3$ and BC influenced the fluorescence parameters of DOM at the end of composting, allowing for a further evaluation of the effect of Fe/BC co-conditioning in composting. The results indicated that BIX and HIX values of DOM in F1, F3, F1 + B15, and F3 + B15 treatments increased significantly by 18.9–25.1% and 4.4–18.5% ($P < 0.05$) (Fig. 5c) when compared to the CK. Among these treatments, F3 displayed the highest BIX value of 0.65, while F3 + B15 showed the highest HIX value of 1.05. On the other hand, the FI (Fluorescence Index) values in F1, F3, and F1 + B15 treatments showed no significant difference when compared to the CK. The HIX value serves as a measure of the degree of humification of DOM, where higher values indicate a more complex molecular composition with increased contents of humus substances and macromolecular compounds (Halbedel and Herzsprung 2020). This observation reflects that Fe/BC co-conditioner can enhance the degree of DOM humification.

3.5 Nitrification genes abundance during Fe/BC co-conditioning composting

The changes in the expression of nitrification-related genes (AOA and AOB) during the composting process are depicted in Fig. 6. During the high-temperature phase of composting, the copy number of AOA genes was significantly lower in F1, F3, F1 + B15, and F3 + B15 compared to CK (Fig. 6a). This decrease might be attributed to the acidic environment inhibiting the growth and activity of ammonia-oxidizing bacteria. However, by the end of composting, the copy number of AOA genes in F1 + B15 and F3 + B15 was significantly higher than that in CK ($P < 0.05$). This outcome can be attributed to the porous structure of biochar, which provides a suitable environment for microorganisms to multiply and facilitates NH_3 oxidation. Additionally, the abundant acidic functional groups on the biochar surface effectively absorb NH_4^+ and promote the ammonia oxidation process.

As shown in Fig. 6b, by the end of composting, the copy number of AOB genes in F1, F3, F1 + B15, and F3 + B15 increased by 37.6%, 42.3%, 65.8%, and 170.5%, respectively, compared to the CK treatment. These results indicate that the addition of Fe/BC conditioner enhanced the copy number of nitrifying bacteria, consequently reducing NH_3 emissions from the composting process.

3.6 *NH_3 reduction mechanisms and correlation analysis*

To analyze the relationship between NH_3 emissions in Fe/BC co-conditioning composting and properties, a structural equation model analysis was conducted in

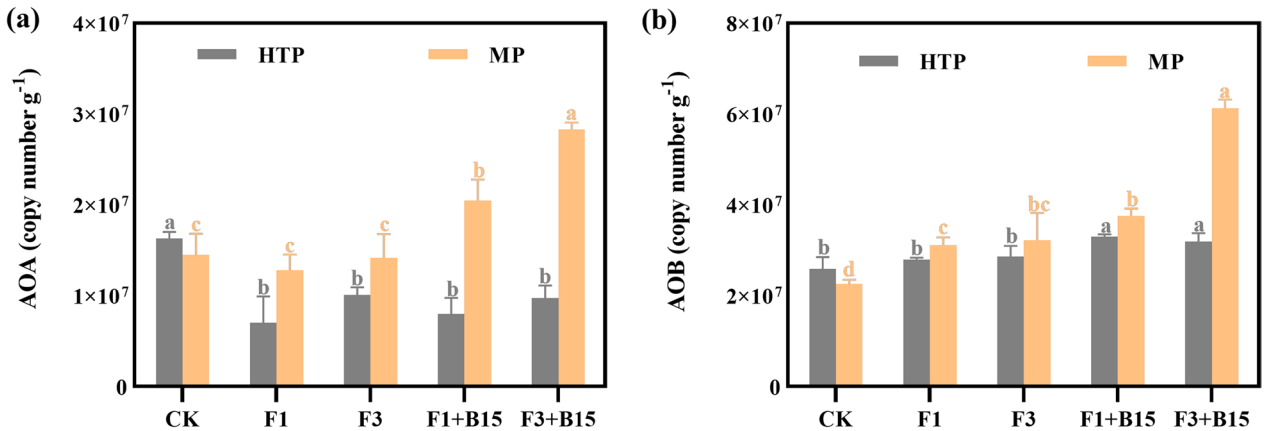

Fig. 6 **a** Copy number of AOA genes and **b** copy number of AOB genes during the composting process. Data are mean ± SD (n = 3)

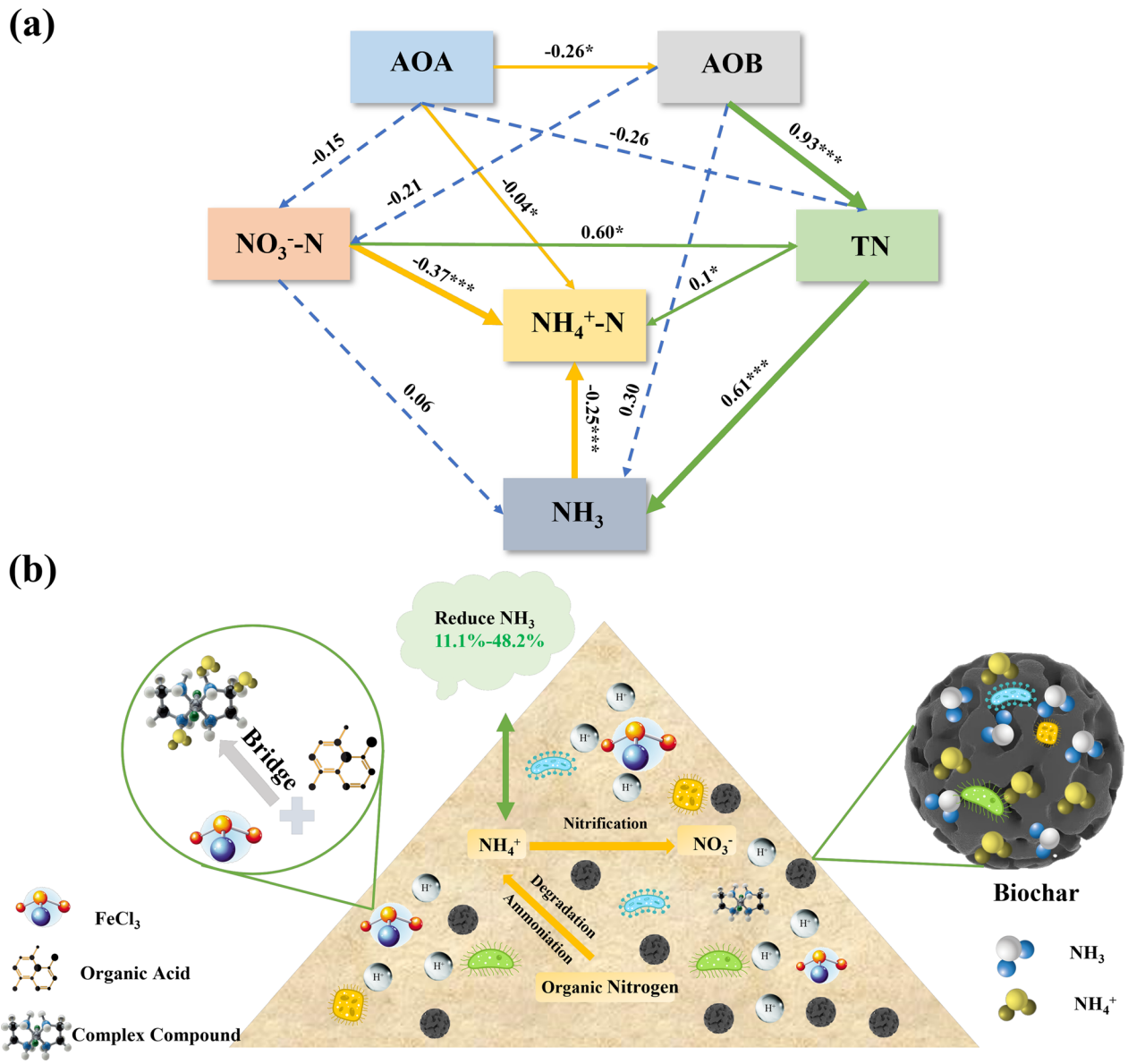

Fig. 7 **a** Structural equation model between NH_3 character indexes (the dashed blue line indicates no significance; the solid green line indicates a positive association; the solid yellow line indicates a negative association, * $P<0.05$; *** $P<0.001$), **b** schematic diagram of the mechanism of Fe/BC co-conditioning to reduce NH_3 emissions

this study, and the results are presented in Fig. 7a. NH_3 emissions were found to be positively correlated with TN ($P<0.001$) but negatively correlated with NH_4^+ ($P<0.001$). This can be attributed to the addition of Fe/BC co-conditioner, which absorbs more NH_4^+ during composting, inhibiting the conversion of NH_4^+ to NH_3. Furthermore, the copy number of AOA genes displayed a significant negative correlation with NH_4^+ ($P<0.05$), while the copy number of AOB genes showed a significant positive correlation with TN ($P<0.001$). These results suggest that the increase in TN content in composting, caused by the addition of Fe/BC co-conditioners, is associated with the copy number of AOB genes.

The potential mechanism underlying the reduction of NH_3 emissions through Fe/BC co-conditioning is summarized in Fig. 7b. The hydrolysis of $FeCl_3$ produces a large amount of H^+, reducing the pH value of the composting. This, in turn, inhibits microbial activity and decreases the decomposition rate of organic matter, thereby inhibiting NH_3 production. Moreover, Fe^{3+} can react with the reducing groups (-OH, -COOH) on the

surface of FA in the composting, forming compounds via a bridging effect that absorbs NH_4^+ and further reduces NH_3 emissions (Nahm 2003).

Additionally, the reduction of NH_3 emissions attributed to the addition of biochar is linked to its high specific surface area and porous structure. Agyarko-Mintah et al. (2017) demonstrated that NH_3 adsorption mainly occurs in the pore space of biochar. Furthermore, the abundant acid functional groups on the biochar surface effectively adsorb NH_4^+ and NH_3, enhancing nitrification and reducing NH_3 emissions (Khan et al. 2020). Moreover, biochar increases cellulase activity during composting, leading to more soluble organic carbon from cellulose decomposition. This, in turn, improves the utilization of NH_4^+ by microorganisms and ultimately reduces NH_3 emissions (Yin et al. 2023).

3.7 Environmental and economic benefit analysis of Fe/BC co-conditioning

Evaluating the benefits of conditioners for composting is important, but there is a lack of relevant research. To compare the advantages and disadvantages of Fe/BC co-conditioners with CK, a preliminary economic benefit analysis was conducted, taking into consideration both costs and income. The inputs involved in the calculation were mainly $FeCl_3$ and the amount of biochar used, while the outputs mainly included enhanced fertilizer value and reduced NH_3 emission benefits. The net benefit was determined as the difference between the inputs and outputs.

The costs of $FeCl_3$, biochar, inorganic fertilizer, and reduced NH_3 emissions are shown in Additional file 1: Table S3a. Additionally, the economic and environmental benefits of adding Fe/BC co-conditioners compared to CK are shown in Additional file 1: Table S3b. Among the treatments, F1 had the lowest economic benefit at 0.1 \$ t^{-1}, while the F3 + B15 treatment had the highest economic benefit at 23.6 \$ t^{-1}. This indicates that the economic benefit of using both $FeCl_3$ and biochar is superior to that of using $FeCl_3$ alone. Considering that the total amount of NH_3 produced by livestock in China was about 5.5×10^9 kg N (Zhang et al. 2020), the reduction in NH_3 achieved by adding Fe/BC co-conditioners ranged from 11.1% to 48.2%. If Fe/BC co-conditioners were widely adopted for treating livestock manure in China, it could theoretically generate an economic and environmental benefit of 0.4–1.2 billion \$ $year^{-1}$.

However, the economic and environmental benefit analysis in this study was relatively preliminary. Firstly, it only considered the effect of Fe/BC conditioners on NH_3 reduction, while other greenhouse gases like N_2O and CH_4 were not taken into account. Secondly, the reduction of NH_3 emissions also has potential benefits for human health and ecosystem health, but these economic benefits were not assessed in this study. Furthermore, certain parameters of the composting process, such as the cost of composting raw materials, site fees, and labor costs, were not included due to varying market prices in each country. Future studies should quantify these parameters by collecting relevant data to provide a more comprehensive economic analysis.

4 Future research

This study focused on the relationship between Fe/BC co-conditioners on physicochemical properties and NH_3 emissions in aerobic composting. In future studies, further research is needed to investigate the interactions between microbial communities in aerobic composting with the addition of Fe/BC co-conditioners, especially the relationship between Fe/BC co-conditioners on the functional N-converting flora. In addition, the potential environmental risks of Fe/BC co-conditioners should be kept in mind during their application. This study did not discuss the possible increased risk of soil-borne disease transmission by Fe addition and its long-term effects on crop growth, and future analyses of the interactions between soil, microbes and crops with Fe/BC organic manures need to be further strengthened.

5 Conclusion

In this study, we investigated the effects of Fe/BC co-conditioners on NH_3 emissions, physical and chemical properties, nutrient dynamics, and humus and organic matter contents. The results of this study show that Fe/BC co-conditioning created an acidic environment that resulted in a significant reduction of cumulative NH_3 emissions during the high temperature period of the composting process. Moreover, the addition of Fe/BC co-conditioners facilitated the absorption of NH_4^+–N and NO_3^-–N in the composting process through adsorption, effectively inhibiting NH_3 emissions. Fe/BC co-conditioning also reacted with the reducing substances in composting, which had a positive effect on the degradation of organic matter and humic acid, and improved the humification index of DOM. Comparative analysis with traditional organic compost demonstrated that the incorporation of Fe/BC co-conditioners generated more substantial economic and environmental benefits. Overall, this study highlights the effectiveness of Fe/BC co-conditioning in reducing NH_3 emissions and enhancing composting quality. As a promising approach for the reduction and harmless utilization of manure, it holds tremendous potential for widespread application. However, when Fe/BC organic fertilizers are applied in field trials, there is

a need to observe the long-term effects on crops and to carry out risk assessments.

Supplementary Information

The online version contains supplementary material available at https://doi.org/10.1007/s42773-023-00295-x.

Additional file 1: Table S1. Initial physical and chemical properties of composting materials. **Table S2.** Content of partial metal ions in finished compost. **Table S3a.** The price of Fe/BC co-conditioners and fertilizer ($/t). **Table S3b.** The economic and environment benefits of adding Fe/BC conditioners compared with organic fertilizer ($/t). **Figure S1.** XRD patterns and Fourier infrared spectra of biochar. **Figure S2.** The fluorescence spectra of DOM in composting samples were obtained based on PARAFAC analysis. **Figure S3.** FTIR analysis of the functional groups of the different treatments. **Figure S4.** 2D-COS FTIR analysis of the functional groups of the different treatments.

Acknowledgements
We thank Mr. Yingjie Zhao for assisting with the sample collection.

Author contributions
JW: writing-original draft; investigation; methodology. HX: investigation; writing-reviewing & editing; supervision. JW: methodology. WH: writing-reviewing & editing. XZ: writing-reviewing & editing. JH: writing-reviewing & editing. YF: conception; writing-reviewing & editing; supervision. LX: writing-review & editing. The author(s) read and approved the final manuscript.

Funding
This work was funded by National Key Research and Development Program of China (2021YFD1700805), the National Natural Science Foundation of China (No. 42277332), Natural Science Foundation of Jiangsu Province (SBK2022022675) and Yunnan Branch of China National Tobacco Corporation (2022530000241022). Y. F. Feng thanks the support of "333" High-level Talents Training Project of Jiangsu Province (2022-3-23-083).

Data availability
All data generated or analyzed during this study are included in this published article and its Additional files.

Declarations

Competing interests
The authors have no relevant financial or non-financial interests to disclose.

Author details
[1]Key Laboratory of Agro-Environment in Downstream of Yangtze Plain, Ministry of Agriculture and Rural Affairs, Institute of Agricultural Resources and Environment, Jiangsu Academy of Agricultural Sciences, Nanjing 210014, China. [2]Jiangsu Key Laboratory of Chemical Pollution Control and Resources Reuse, School of Environmental and Biological Engineering, Nanjing University of Science and Technology, Nanjing 210094, China. [3]Key Laboratory of Integrated Regulation and Resources Development of Shallow Lakes, Ministry of Education, College of Environment, Hohai University, Nanjing 210098, China.

Received: 17 August 2023 Revised: 18 December 2023 Accepted: 23 December 2023
Published online: 09 January 2024

References

Agyarko-Minta E, Cowie A, Van Zwieten L, Singh BP, Smillie R, Harde S, Fornasier F (2017) Biochar lowers ammonia emission and improves nitrogen retention in poultry litter composting. Waste Manag 61:129–137. https://doi.org/10.1016/j.wasman.2016.12.009

Awasthi MK, Pandey AK, Bundela PS, Wong JWC, Li RH, Zhan ZQ (2016) Co-composting of gelatin industry sludge combined with organic fraction of municipal solid waste and poultry waste employing zeolite mixed with enriched nitrifying bacterial consortium. Bioresour Technol 213:181–189. https://doi.org/10.1016/j.biortech.2016.02.026

Awasthi MK, Wang MJ, Chen HY, Wang Q, Zhao JC, Ren XN, Li DS, Awasthi SK, Shen F, Li RH, Zhang ZQ (2017) Heterogeneity of biochar amendment to improve the carbon and nitrogen sequestration through reduce the greenhouse gases emissions during sewage sludge composting. Bioresour Technol 224:428–438. https://doi.org/10.1016/j.biortech.2016.11.014

Bartos JM, Boggs BL, Falls JH, Siegel SA (2014) Determination of phosphorus and potassium in commercial inorganic fertilizers by inductively coupled plasma-optical emission spectrometry: single-laboratory validation. J AOAC Int 97:687–699. https://doi.org/10.5740/jaoacint.12-399

Cao YB, Wang X, Bai ZH, Chadwick D, Misselbrook T, Sommer GS, QinMa WL (2019) Mitigation of ammonia, nitrous oxide and methane emissions during solid waste composting with different additives: a meta-analysis. J Clean Prod 235:626–635. https://doi.org/10.1016/j.jclepro.2019.06.288

Cao YB, Wang X, Liu L, Velthof GL, Misselbrook T, Bai ZH, Ma L (2020) Acidification of manure reduces gaseous emissions and nutrient losses from subsequent composting process. J Environ Manage 264:110454. https://doi.org/10.1016/j.jenvman.2020.110454

Chan MT, Selvam A, Wong JWC (2016) Reducing nitrogen loss and salinity during 'struvite' food waste composting by zeolite amendment. Bioresour Technol 200:838–844. https://doi.org/10.1016/j.biortech.2015.10.093

Chen PZ, Zheng XQ, Cheng WM (2022) Biochar combined with ferrous sulfate reduces nitrogen and carbon losses during agricultural waste composting and enhances microbial diversity. Process Saf Environ Prot 162:531–542. https://doi.org/10.1016/j.psep.2022.04.042

Chung WJ, Chang SW, Chaudhary DK, Shin JD, Kim H, Karmegam N, Govarthanan M, Chandrasekaran M, Ravindran B (2021) Effect of biochar amendment on compost quality, gaseous emissions and pathogen reduction during in-vessel composting of chicken manure. Chemosphere 283:131129. https://doi.org/10.1016/j.chemosphere.2021.131129

De Melo BAG, Motta FL, Santana MHA (2016) Humic acids: Structural properties and multiple functionalities for novel technological developments. Mater Sci Eng C 62:967–974. https://doi.org/10.1016/j.msec.2015.12.001

Ding Y, Wei JJ, Xiong JS, Zhou BW, Cai HJ, Zhu WQ, Zhang HJ (2019) Effects of operating parameters on in situ NH_3 emission control during kitchen waste composting and correlation analysis of the related microbial communities. Environ Sci Pollut Res 26:11756–11766. https://doi.org/10.1007/s11356-019-04605-4

Gómez-Brandón M, Lazcano C, Domínguez J (2008) The evaluation of stability and maturity during the composting of cattle manure. Chemosphere 70:436–444. https://doi.org/10.1016/j.chemosphere.2007.06.065

Greff B, Szigeti J, Nagy ÁN, Lakatos E, Varga L (2022) Influence of microbial inoculants on co-composting of lignocellulosic crop residues with farm animal manure: A review. J Environ Manage 302:114088. https://doi.org/10.1016/j.jenvman.2021.114088

Halbedel S, Herzsprung P (2020) Short communication on "Differentiating with fluorescence spectroscopy the sources of dissolved organic matter in soils subjected to drying" [Zsolnay et al. Chemosphere 38, 45–50, 1999]. Chemosphere 239: 124818. https://doi.org/10.1016/j.chemosphere.2019.124818

Jiang T, Schuchardt F, Li GX, Guo R, Zhao YQ (2011) Effect of C/N ratio, aeration rate and moisture content on ammonia and greenhouse gas emission during the composting. J Environ Sci 23:1754–1760. https://doi.org/10.1016/S1001-0742(10)60591-8

Karlsson T, Persson P (2012) Complexes with aquatic organic matter suppress hydrolysis and precipitation of Fe(III). Chem Geol 322–323:19–27. https://doi.org/10.1016/j.chemgeo.2012.06.003

Khan N, Clark I, Sánchez-Monedero MA, Shea S, Meier S, Bolan N (2014) Maturity indices in co-composting of chicken manure and sawdust with biochar. Bioresour Technol 168:245–251. https://doi.org/10.1016/j.biortech.2014.02.123

Khan MB, Cui XQ, Jilani G, Tang L, Lu M, Cao XR, Sahito ZA, Hamid Y, Hussain B, Yang XE, He ZL (2020) New insight into the impact of biochar during vermi-stabilization of divergent biowastes: literature synthesis and research pursuits. Chemosphere 238:124679. https://doi.org/10.1016/j.chemosphere.2019.124679

Kianirad M, Muazardalan M, Savaghebi G, Farahbakhsh M, Mirdamadi S (2010) Effects of temperature treatment on corn cob composting and reducing of composting time: a comparative study. Waste Manag Res J Sustain Circ Econ 28:882–887. https://doi.org/10.1177/0734242X09342359

Kuroda K, Waki M, Yasuda T, Fukumoto Y, Tanaka A, Nakasaki K (2015) Utilization of *Bacillus* sp. strain TAT105 as a biological additive to reduce ammonia emissions during composting of swine feces. Biosci Biotechnol Biochem 79:1702–1711. https://doi.org/10.1080/09168451.2015.1042831

Li CN, Li HY, Yao T, Su M, Ran F, Li JH, He L, Chen X, Zhang C, Qiu HZ (2021) Effects of swine manure composting by microbial inoculation: Heavy metal fractions, humic substances, and bacterial community metabolism. J Hazard Mater 415:125559. https://doi.org/10.1016/j.jhazmat.2021.125559

Liu N, Zhou JL, Han LJ, Ma SS, Sun XX, Huang GQ (2017) Role and multi-scale characterization of bamboo biochar during poultry manure aerobic composting. Bioresour Technol 241:190–199. https://doi.org/10.1016/j.biortech.2017.03.144

Liu Y, Liu JW, Zheng GD, Yang JX, Cheng Y (2022) Inhibitory Effects of appropriate addition of zero-valent iron on NH_3 and H_2S emissions during sewage sludge composting. Agriculture 12:2002. https://doi.org/10.3390/agriculture12122002

López-González JA, López MJ, Vargas-García MC, Suárez-Estrella F, Jurado M, Moreno J (2013) Tracking organic matter and microbiota dynamics during the stages of lignocellulosic waste composting. Bioresour Technol 146:574–584. https://doi.org/10.1016/j.biortech.2013.07.122

Luo YM, Xu DG, Li GX (2013) Effect of superphosphate as additive on nitrogen and carbon losses during pig manure composting. Appl Mech Mater 295–298:1675–1679. https://doi.org/10.4028/www.scientific.net/AMM.295-298.1675

Mei J, Ji K, Su LH, Wu MT, Zhou XJ, Duan ES (2021) Effects of $FeSO_4$ dosage on nitrogen loss and humification during the composting of cow dung and corn straw. Bioresour Technol 341:125867. https://doi.org/10.1016/j.biortech.2021.125867

Nahm KH (2003) Current pollution and odor control technologies for poultry production. Avian Poult Biol Rev 14:151–174. https://doi.org/10.3184/147020603783637472

Proietti P, Calisti R, Gigliotti G, Nasini L, Regni L, Marchini A (2016) Composting optimization: integrating cost analysis with the physical-chemical properties of materials to be composted. J Clean Prod 137:1086–1099. https://doi.org/10.1016/j.jclepro.2016.07.158

Qian XY, Shen GX, Wang ZQ, Guo CX, Liu YQ, Lei ZF, Zhang ZY (2014) Co-composting of livestock manure with rice straw: characterization and establishment of maturity evaluation system. Waste Manag 34:530–535. https://doi.org/10.1016/j.wasman.2013.10.007

Shan YN, Chen JH, Wang L, Li F, Fu XH, Le YQ (2013) Influences of adding easily degradable organic waste on the minimization and humification of organic matter during straw composting. J Environ Sci Health Part B 48:384–392. https://doi.org/10.1080/03601234.2013.742391

Shan GC, Xu JQ, Jiang ZW, Li MQ, Li QL (2019) The transformation of different dissolved organic matter subfractions and distribution of heavy metals during food waste and sugarcane leaves co-composting. Waste Manag 87:636–644. https://doi.org/10.1016/j.wasman.2019.03.005

Shan GC, Li WG, Gao YJ, Tan W, Xi BD (2021) Additives for reducing nitrogen loss during composting: a review. J Clean Prod 307:127308. https://doi.org/10.1016/j.jclepro.2021.127308

Shi MZ, Zhao XY, Zhu LJ, Wu JQ, Mohamed TA, Zhang X, Chen XM, Zhao Y, Wei ZM (2020) Elucidating the negative effect of denitrification on aromatic humic substance formation during sludge aerobic fermentation. J Hazard Mater 388:122086. https://doi.org/10.1016/j.jhazmat.2020.122086

Smebye A, Alling V, Vogt RD, Gadmar TC, Mulder J, Cornelissen G, Hale SE (2016) Biochar amendment to soil changes dissolved organic matter content and composition. Chemosphere 142:100–105. https://doi.org/10.1016/j.chemosphere.2015.04.087

Sudharsan Varma V, Kalamdhad AS (2015) Evolution of chemical and biological characterization during thermophilic composting of vegetable waste using rotary drum composter. Int J Environ Sci Technol 12:2015–2024. https://doi.org/10.1007/s13762-014-0582-3

Usman M, Chen HH, Chen KF, Ren S, Clark JH, Fan JJ, Luo G, Zhang SC (2019) Characterization and utilization of aqueous products from hydrothermal conversion of biomass for bio-oil and hydro-char production: a review. Green Chem 21:1553–1572. https://doi.org/10.1039/C8GC03957G

Wang Q, Li RH, Cai HZ, Awasthi MK, Zhang ZQ, Wang JJ, Ali A, Amanullah M (2016) Improving pig manure composting efficiency employing Ca-bentonite. Ecol Eng 87:157–161. https://doi.org/10.1016/j.ecoleng.2015.11.032

Wang XK, Chen TB, Zheng GD (2020) Preservation of nitrogen and sulfur and passivation of heavy metals during sewage sludge composting with KH_2PO_4 and $FeSO_4$. Bioresour Technol 297:122383. https://doi.org/10.1016/j.biortech.2019.122383

Wong JWC, Fang M (2000) Effects of lime addition on sewage sludge composting process. Water Res 34:3691–3698. https://doi.org/10.1016/s0043-1354(00)00116-0

Xiao R, Awasthi MK, Li RH, Park J, Pensky SM, Wang Q, Wang JJ, Zhang ZQ (2017) Recent developments in biochar utilization as an additive in organic solid waste composting: a review. Bioresour Technol 246:203–213. https://doi.org/10.1016/j.biortech.2017.07.090

Yang YJ, Awasthi MK, Du W, Ren XN, Lei T, Lv JL (2020) Compost supplementation with nitrogen loss and greenhouse gas emissions during pig manure composting. Bioresour Technol 297:122435. https://doi.org/10.1016/j.biortech.2019.122435

Yang Y, Wang GY, Li GX, Ma RN, Kong YL, Yuan J (2021) Selection of sensitive seeds for evaluation of compost maturity with the seed germination index. Waste Manag 136:238–243. https://doi.org/10.1016/j.wasman.2021.09.037

Yin YN, Li MT, Tao XH, Yang C, Zhang WR, Li HC, Zheng YC, Wang XC, Chen R (2023) Biochar enhanced organic matter transformation during pig manure composting: Roles of the cellulase activity and fungal community. J Environ Manage 333:117464. https://doi.org/10.1016/j.jenvman.2023.117464

Zhang HY, Li GX, Wei HF (2013) Influence of aeration on NH_3, CH_4 and N_2O emissions during kitchen waste composting. Adv Mater Res 864–867:1904–1908. https://doi.org/10.4028/www.scientific.net/AMR.864-867.1904

Zhang HY, Li GX, Yang JB, Yang QY (2014) Effect of co-composting of kitchen waste and agricultural waste on H_2S and NH_3 emission. Appl Mech Mater 448–453:741–745. https://doi.org/10.4028/www.scientific.net/AMM.448-453.741

Zhang Y, Zhao Y, Chen YN, Lu Q, Li MX, Wang XQ, Wei YQ, Xie XY, Wei ZM (2016) A regulating method for reducing nitrogen loss based on enriched ammonia-oxidizing bacteria during composting. Bioresour Technol 221:276–283. https://doi.org/10.1016/j.biortech.2016.09.057

Zhang XM, Gu BJ, Van Grinsven H, Lam SK, Liang X, Bai M, Chen DL (2020) Societal benefits of halving agricultural ammonia emissions in China far exceed the abatement costs. Nat Commun 11:4357. https://doi.org/10.1038/s41467-020-18196-z